Ab initio studies of stationary points of the Al₂O₃ molecule

Ch. Chang[1,a], A.B.C. Patzer[1], E. Sedlmayr[1], and D. Sülzle[2]

[1] Institut für Astronomie und Astrophysik, Technische Universität Berlin, Hardenbergstr. 36, 10623 Berlin, Germany
[2] Schering AG Research Laboratories, 13342 Berlin, Germany

Abstract. We report a theoretical *ab initio* investigation on energetically low-lying stationary points of the Al_2O_3 molecular system. The calculations were performed at the Hartree-Fock (HF) and second-order Møller-Plesset (MP2) frozen core level of approximation using the standard 6-31G(d) basis set. Several isomeric singlet as well as higher spin states of Al_2O_3 which lie close to each other within an energy range of about 8 eV (at MP2) are characterised. The lowest of these stationary points is in fact a triplet state of planar C_{2v} symmetry. It is by 0.08 eV (MP2) lower than the often discussed linear $D_{\infty h}$ singlet state. Atomisation energies for all species are quite large showing that the system is strongly bound. Energies, harmonic vibrational modes, and geometric parameters are compared with the results of earlier work by Solomonik and Sliznev [1], Nemukhin and Weinhold [2], Andrews *et al.* [3] and Desai *et al.* [4]. Based on our calculations we give a tentative assignment of some selected vibrational wave numbers and an interpretation of some features of the photoelectron spectrum.

PACS. 33.15.-e Properties of molecules and molecular ions – 31.15.Ar Ab initio calculations

1 Introduction

Small aluminium-oxygen systems Al_nO_m ($n = 1-4; m = 1-5$) and clusters thereof are important in many areas of physics such as in explorations of properties of ceramic materials [5–7] or in studies of interfacial processes in surface science [8]. Therefore there has been considerable interest in these systems, both from an experimental [9–13] and theoretical [14–25] point of view, all of which disclose an amazingly rich structural diversity of strongly bound neutral and charged isomers. However for Al_2O_3 apart from an extensive literature about various phases of the solid and liquid state [26–30] only few articles *viz.* by Solomonik and Sliznev [1], Nemukhin and Weinhold [2], Andrews *et al.* [3] and Desai *et al.* [4] are known to us, which treat the isolated Al_2O_3 molecule in more detail.

From an astrophysical point of view these systems are intriguing because when considering the cosmic abundances of the elements Al and O [31], clusters of aluminium oxides, *e.g.* Al_2O_3 which is the stoichiometric composition of the known solid corundum [26,28,29], could play an important role in dust formation processes from the gas phase in circumstellar shells of oxygen rich stars [32–38]. For a study of this kind of processes information about thermodynamical and energetic properties of the gas phase species is required. Unfortunately often these data cannot be found in standard reference works and tables for the relevant molecular species. In this case

theoretical computation is the only possibility to obtain at least some estimates of the desired quantities.

In this paper we therefore have a closer look at the electronic structure properties of the Al_2O_3 molecule using standard *ab initio* techniques. In a subsequent article these calculated data will be used to determine thermodynamical functions of gas phase Al_2O_3.

2 Computational aspects

For all computations we made use of the Gaussian 92/DFT system of programs [39]. The chosen basis set is of standard 6-31G(d) type [40] which in this case consists of 83 basis functions and 188 primitives. In this basis all geometric structures were fully optimised at both Hartree-Fock (HF) and second-order Møller-Plesset (MP2) frozen core level of approximation [40]. The calculated wave numbers of the various harmonic vibrational modes were scaled by 0.8929 (HF) and 0.9434 (MP2) [41] where appropriate. For singlet states all calculated molecular quantities given are restricted HF (RHF) values while for higher spin states unrestricted HF (UHF) was used. Inspection of the expectation values $\langle \hat{S}^2 \rangle$, however, indicates that spin contamination is always very small.

Reference energies of the free atoms were calculated at both ROHF (ROMP2) and UHF (UMP2) level of approximation. Fortunately, the difference of the total energy of the 2 Al (^2P_u) and 3 O (^3P_g) ground state asymptote at the ROMP2 and the UMP2 level is at best only 0.025 eV

[a] e-mail: `chang@alt.physik.Tu-Berlin.de`

so that ROHF and ROMP2 total atomic energies are used as reference in the calculation of the atomisation energies D_{at} for closed-shell, and UHF and UMP2 energies for open-shell species. According to

$$D_{at} = \left(\sum_{atoms} E_M^{tot}(atoms) \right) - E_M^{tot}(molecule) \quad (1)$$

where M = Restricted HF(MP2) for a singlet molecular state or M = Unrestricted HF(MP2) otherwise. The experimentally observable quantity then is

$$D_0 = D_{at} - E_{ZP} \quad (2)$$

where E_{ZP} is the zero point vibrational energy.

In the frequency calculations the vibrational wave numbers $\tilde{\nu}_k$ were computed in the harmonic approximation. The integrated absorption coefficients A_k for strictly harmonic motion are then given by

$$A_k = \int_\nu \epsilon_k(\nu) d\nu = \frac{\pi}{3c} \left| \left(\frac{\partial \boldsymbol{\mu}}{\partial Q_k} \right)_0 \right|^2 \quad (3)$$

where c is the speed of light, $\boldsymbol{\mu}$ the electric dipole moment, and Q_k the normal coordinate of the k-th vibrational mode. The linear absorption coefficient ϵ is macroscopically defined by the intensity relation

$$dI(\nu) = -\epsilon(\nu) n_0 I(\nu) dl \quad (4)$$

where n_0 is the number density of the particles in $[cm^{-3}]$.

3 Results and discussion

In a first series of calculations we determined the low-lying stationary points at the HF level of approximation, thereby sampling a wide range of nuclear configurations. This resulted in 13 singlet and higher spin structures which are labelled systematically by ^{1}1, ^{3}2, and so on, where the superscript indicates spin multiplicity. These 13 isomers can be allotted to 7 different geometric nuclear configurations illustrated in Figure 1. A diagrammatic representation of the calculated total energies is given in Figure 2.

Three structures need special mentioning: ^{1}6 is in fact a transition structure with one imaginary wave number at HF level of theory while it turns out to be a true minimum at MP2. ^{1}8$_{HF}$ (C$_{2v}$, kite-shaped) is a minimum at HF but distorts to a form of lower symmetry (C$_s$, curved) at MP2 which is ^{1}5 in our nomenclature. ^{3}2*, however, which at first sight looked like a minimal point, after further inspection proved not to be a stable structure neither at HF nor at the correlated level. The calculated b_2 normal mode of 3317 cm^{-1} at the HF level together with its unusual high integrated absorption coefficient of 5×10^{-5} cm^2 s^{-1}
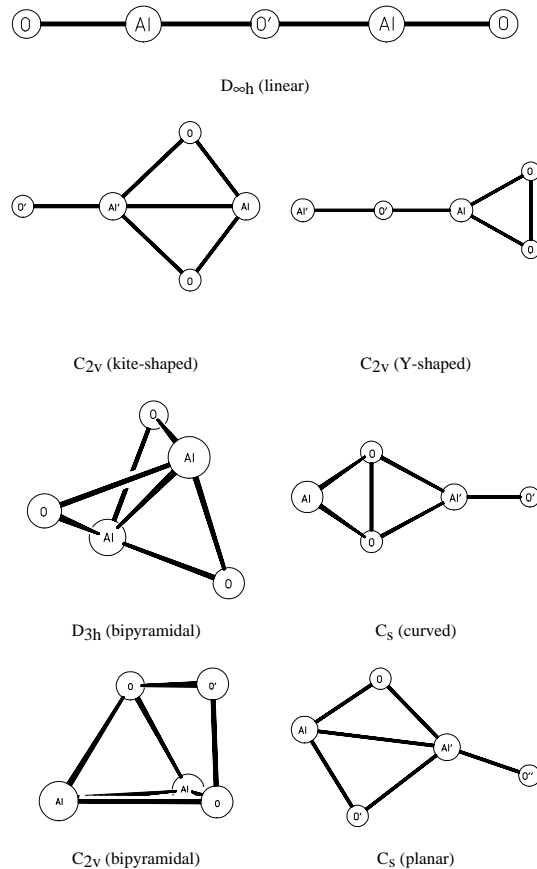

Fig. 1. Geometric nuclear configurations of stable Al$_2$O$_3$ isomers.

indicated that the wave function is probably not stable with respect to the internal degrees of freedom. A stability analysis of the wave function and further geometry optimisation gave rise to two other triplet species *viz.* ^{3}2 and ^{3}7, that are both minima and lower in energy than the structure ^{3}2*. ^{3}2 is indeed the lowest point of all we found and surprisingly stays lowest even at MP2 level, where it is by 0.08 eV lower than the well known linear ^{1}1. This could well emanate from a UHF effect, because the greater flexibility of an unrestricted wave function necessarily causes a lowering in energy within the variational SCF part. Albeit structures ^{1}1 and ^{3}2 will stay vitally similar in energy delineating the two most stable isomeric species of this system. All other points represent true local minima with all eigenvalues of the Hessian matrix being positive.

We regard the HF approximation only as a first step to a more appropriate description of the molecular system. This is sustained by some supplementary studies on the most stable ground state structures of AlO and Al$_2$O for which the relevant data can be found in the literature (see *e.g.* [10,42–44]). Comparison between HF and MP2 results evinces that atomisation energies are indeed very poor for HF and in good agreement for MP2. Whereas discrepancies in geometric parameters are in general quite small. It
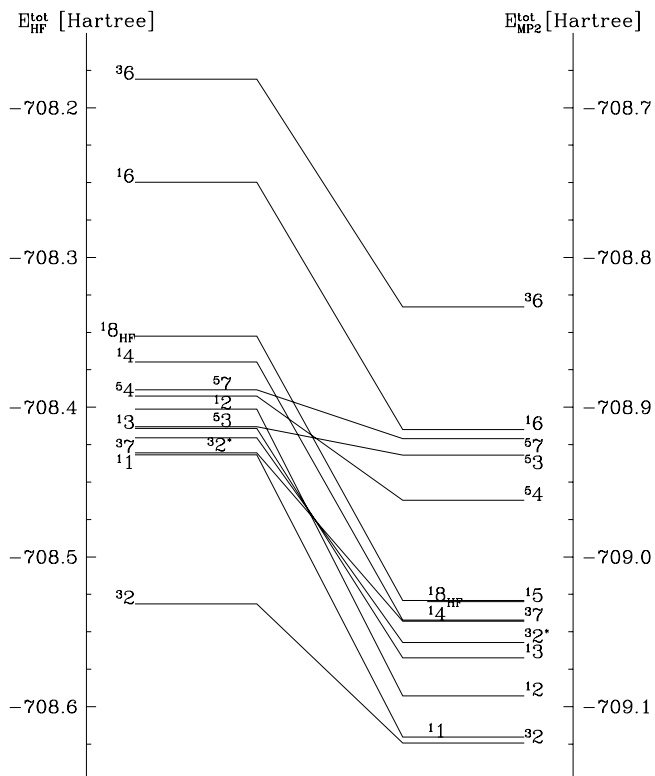
Fig. 2. Hartree-Fock and second-order Møller-Plesset total energies.

follows that for an adequate determination of atomisation energies it is definitely important to include electron correlation. Amidst various possibilities that allow for taking electron correlation into account the choice of MP2 is one of the least expensive and at the same time one of the most efficient. A comparison of different post-HF methods has recently been given by Helgaker *et al.* [45].

This can also be concluded from a very thorough study of the aluminium oxides Al_nO ($n = 1-4$) by Boldyrev and Schleyer [20]. They present a comparison of the experimentally determined ground state structures and energies of atomisation and the corresponding calculated values at the UHF and UMPn ($n = 2-4$) level for the well characterised aluminium oxides AlO and Al_2O in the gas phase. Their results show a clear preference for the UMP2 approach. The deviation of the experimental and calculated internuclear distances at the UHF and UMP2 level are 0.079 Å and 0.03 Å for AlO and 0.027 Å and 0.003 Å for Al_2O. The calculated D_{at} values for AlO vary between 2.27 eV at the UHF level of theory and 4.18 eV at UMP4. In this series the UMP2 calculation gives rise to a D_{at} of 4.21 eV. The experimentally determined value of D_0 is 5.26 eV [43]. The same holds true for Al_2O. D_{at} values of 7.22 eV and 10.71 eV were computed at the UHF and UMP2 level, respectively, the experimental D_0 being 10.84 eV [43].

Consequently in a second series of calculations we optimised at the correlated MP2 frozen core level all ascertained species with the corresponding HF geometry as starting point. The results thereof are compiled in Table 1,

energies, Table 2, unscaled wave numbers and integrated absorption coefficients, and Table 3, geometries. A look at Figure 2 confirms the well known changes that come about when going from HF to MP2 descriptions *i.e.* energies are lowered and overestimation of open-shell species disappears.

At the MP2 level **⁵3** and **⁵7** are no longer minima. Calculated wave numbers of $34i$ cm⁻¹ (b_1) and $18i$ cm⁻¹ (a'') indicate that both quintet species are in fact transition structures. Albeit the very small magnitudes of the two imaginary wave numbers point to a very flat potential energy hypersurface for the b_1 normal mode of **⁵3** and the a'' vibration of **⁵7**.

There are essentially four articles *viz.* by Solomonik and Sliznev [1], Nemukhin and Weinhold [2], Andrews *et al.* [3], and Desai *et al.* [4], which report *ab initio* studies on the Al_2O_3 molecule, though only the first of these is devoted solely to this system.

Solomonik and Sliznev [1] treat two states *i.e.* structure **¹1** and **¹4** at HF level employing a slightly larger basis than 6-31G(d) for the first and a somewhat smaller for the second. Nonetheless their results on energetic, geometric, and vibrational quantities are perfectly comparable to this work.

Nemukhin and Weinhold [2] likewise use the 6-31G(d) basis set at both HF and MP2 characterising three minimal points *i.e.* **¹1**, **¹3**, and **¹6**. They discard a D_{3h} form as being a transition structure without giving further details. Their presented results are in agreement with ours, except for the **¹6** species which has a small incongruity in energy. Besides we are able to localise an isomer of D_{3h} symmetry *i.e.* **¹4** which is a true minimum at both HF and MP2.

The article by Andrews *et al.* [3] describes a very thorough experimental study on various aluminium oxides. They mention just briefly the **¹1** species treated at HF and MP2 in a double zeta polarisation (DZP) basis.

Desai *et al.* [4] investigated small aluminium oxide clusters by photoelectron spectroscopy. They also report the singlet structures **¹2**, **¹1**, and **¹3** in this energetic order computed at HF and MP2 with the 6-31G(d) basis. Yet, the authors do not explicitly adduce any total energies. From their experimental results they infer a rhombic geometry for the ground state of Al_2O_3. Their calculated vibrational data accord as well with this work.

There is a number of experimentally oriented publications in which the Al_2O_3 system is generated in inert gas matrices at low temperatures. IR and Raman studies were performed and analysed in terms of the possible presence of **¹1** and another unidentified isomer.

Rozhanskii *et al.* [12] reported about the presence of two isomers of Al_2O_3 from the reaction Al + ¹⁶,¹⁸O₂ in low-temperature nitrogen matrices. After photolysis at 10−15 K they assign bands in the IR spectra of the reaction products at 1101 cm⁻¹ and 502 cm⁻¹ to **¹1**. A band at 964 cm⁻¹ is designated to an unknown Al_2O_3 species of C_1 symmetry.

The products of the reaction Al + ¹⁶,¹⁸O₂ in low-temperature nitrogen matrices were also studied by

Table 1. Second-order Møller-Plesset energies [a].

Label	Symmetry	State	$E_{\mathrm{MP2}}^{\mathrm{tot}}$ [Hartree]	$E_{\mathrm{MP2}}^{\mathrm{rel}}$ [eV]	E_{ZP} [b] [eV]	D_{at} [c] [eV]	$\langle \hat{S}^2 \rangle$
$^3\mathbf{2}$	C_{2v} (kite-shaped)	$^3B_2$	-709.124737	0.00	0.31	19.38	2.01
$^1\mathbf{1}$	$D_{\infty h}$ (linear)	$^1\sum_g^+$	-709.120907	0.10	0.29	19.30	
$^1\mathbf{2}$	C_{2v} (kite-shaped)	$^1A_1$	-709.093827	0.84	0.29	18.56	
$^1\mathbf{3}$	C_{2v} (Y-shaped)	$^1A_1$	-709.068879	1.52	0.27	17.88	
$^3\mathbf{2}^{*}$ [d]	C_{2v} (kite-shaped)	$^3B_2$	-709.058823	1.79	1.64	17.58	2.05
$^3\mathbf{7}$	C_s (planar)	$^3A''$	-709.044830	2.17	0.27	17.20	2.01
$^1\mathbf{4}$	D_{3h} (bipyramidal)	$^1A_1'$	-709.044114	2.19	0.30	17.21	
$^1\mathbf{5}$	C_s (curved)	$^1A'$	-709.032053	2.52	0.26	16.88	
$^5\mathbf{4}$	D_{3h} (bipyramidal)	$^5A_2''$	-708.965542	4.33	0.32	15.05	6.08
$^5\mathbf{3}$	C_{2v} (Y-shaped)	$^5B_2$	-708.936027	5.14	0.25	14.24	6.01
$^5\mathbf{7}$	C_s (planar)	$^5A''$	-708.925160	5.43	0.25	13.95	6.02
$^1\mathbf{6}$	C_{2v} (bipyramidal)	$^1A_1$	-708.919197	5.59	0.24	13.81	
$^3\mathbf{6}$	C_{2v} (bipyramidal)	$^3B_2$	-708.838736	7.78	0.43	11.60	2.02

[a] RMP2 energies for singlet and UMP2 energies for higher spin states
[b] zero-point vibrational energy
[c] energy of atomisation (with respect to 2 Al(^2P_u) + 3 O(^3P_g))
[d] $^3\mathbf{2}^*$ turned out not to be a stationary point (*cf.* discussion)

Table 2. Second-order Møller-Plesset wave numbers $\tilde{\nu}_k$ [cm^{-1}], symmetry labels, and integrated absorption coefficients A_k [10^{-8} cm^2 s^{-1}].

Label	$k \longrightarrow$	1	2	3	4	5	6	7	8	9	10
$^3\mathbf{2}$	$\tilde{\nu}_k$	$128(b_1)$	$186(b_2)$	$349(b_1)$	$460(a_1)$	$643(b_2)$	$684(a_1)$	$758(a_1)$	$789(b_2)$	$943(a_1)$	-
	A_k	2.6	8.9	48	0.001	4.3	37	72	80	90	-
$^1\mathbf{1}$	$\tilde{\nu}_k$	$35(\pi_u)$	$35(\pi_u)$	$175(\pi_g)$	$175(\pi_g)$	$251(\pi_u)$	$251(\pi_u)$	$428(\sigma_g^+)$	$925(\sigma_u^+)$	$1132(\sigma_g^+)$	$1240(\sigma_u^+)$
	A_k	9.8	9.8	0	0	56	56	0	53	0	192
$^1\mathbf{2}$	$\tilde{\nu}_k$	$138(b_1)$	$160(b_2)$	$314(b_1)$	$322(b_2)$	$439(a_1)$	$477(a_1)$	$856(a_1)$	$923(b_2)$	$1036(a_1)$	-
	A_k	0.0006	12	44	20	7.5	14	0.05	21	0.04	-
$^1\mathbf{3}$	$\tilde{\nu}_k$	$55(b_1)$	$55(b_2)$	$238(b_2)$	$254(b_1)$	$406(a_1)$	$576(a_1)$	$804(b_2)$	$888(a_1)$	$1141(a_1)$	-
	A_k	2.3	1.1	30	47	14	2.8	24	32	270	-
$^3\mathbf{2}^{*}$	$\tilde{\nu}_k$	$40(b_1)$	$187(b_2)$	$236(b_1)$	$383(a_1)$	$607(b_2)$	$637(a_1)$	$867(a_1)$	$1094(a_1)$	$22430(b_2)$	-
	A_k	0.08	13	36	0.004	40	48	97	39	5000	-
$^3\mathbf{7}$	$\tilde{\nu}_k$	$52(a'')$	$182(a')$	$228(a'')$	$256(a')$	$392(a')$	$603(a')$	$653(a')$	$875(a')$	$1051(a')$	-
	A_k	0.01	10	36	21	5.1	24	49	64	26	-
$^1\mathbf{4}$	$\tilde{\nu}_k$	$337(e'')$	$337(e'')$	$421(e')$	$421(e')$	$576(a_2'')$	$659(e')$	$659(e')$	$687(a_1')$	$796(a_1')$	-
	A_k	0	0	30	30	87	47	47	0	0	-
$^1\mathbf{5}$	$\tilde{\nu}_k$	$60(a')$	$160(a'')$	$211(a')$	$349(a'')$	$421(a')$	$496(a'')$	$605(a')$	$782(a')$	$1117(a')$	-
	A_k	2.0	11	21	22	17	3.0	143	0.03	38	-
$^5\mathbf{4}$	$\tilde{\nu}_k$	$323(e')$	$323(e')$	$426(e'')$	$426(e'')$	$504(a_1')$	$713(a_2'')$	$735(a_1')$	$884(e')$	$884(e')$	-
	A_k	0.00008	0.00008	0	0	0	209	0	170	170	-
$^5\mathbf{3}$	$\tilde{\nu}_k$	$-34(b_1)$	$38(b_2)$	$208(a_1)$	$245(b_2)$	$277(b_1)$	$498(a_1)$	$773(a_1)$	$878(b_2)$	$1107(a_1)$	-
	A_k	0.08	0.05	22	22	52	0.0002	6.1	55	284	-
$^5\mathbf{7}$	$\tilde{\nu}_k$	$-18(a'')$	$181(a')$	$233(a'')$	$302(a')$	$361(a')$	$601(a')$	$650(a')$	$761(a')$	$994(a')$	-
	A_k	0.0006	7.3	46	31	2.2	5.0	95	11	95	-
$^1\mathbf{6}$	$\tilde{\nu}_k$	$69(b_2)$	$146(a_1)$	$231(a_2)$	$309(b_1)$	$398(a_1)$	$447(b_2)$	$629(a_1)$	$759(b_1)$	$838(a_1)$	-
	A_k	0.03	0.005	0	8.6	10	222	2.2	6.1	2.5	-
$^3\mathbf{6}$	$\tilde{\nu}_k$	$194(a_1)$	$267(b_2)$	$317(a_2)$	$461(b_1)$	$483(a_1)$	$585(b_2)$	$686(a_1)$	$1604(b_1)$	$2403(a_1)$	-
	A_k	5.4	1.1	0	15	15	335	5.4	74	41	-

Table 3. Second-order Møller-Plesset geometries (Interatomic distances r_i in [Å] and angles α_i in [deg]; the geometric meaning of these parameters can be inferred from Figure 1).

	r_{AlO}	$r_{Al'O}$	$r_{AlO'}$	$r_{Al'O'}$	$r_{Al'O''}$	α_{OAlO}	$\alpha_{OAl'O}$	$\alpha_{OAlO'}$	$\alpha_{OAl'O'}$	$\alpha_{OAl'O''}$	$\alpha_{O'Al'O''}$
C_{2v} (kite-shaped)											
¹**2**	1.687	1.945		1.639		105.6	87.4		136.3		
³**2**	1.780	1.756		1.755		93.1	94.7		132.6		
³**2***	1.753	1.855		1.629		79.1	74.0		143.0		
C_{2v} (Y-shaped)											
¹**3**	1.724		1.684	1.741		58.6		150.7			
⁵**3**	1.758		1.684	1.725		116.6		121.7			
$D_{\infty h}$ (linear)											
¹**1**	1.629		1.692					180.0			
C_{2v} (bipyramidal)											
¹**6**	2.048		2.233			66.5		41.3			
³**6**	2.004		2.453			65.8		36.9			
C_s (planar)											
³**7**	1.709	1.786	1.894	2.109	1.631			92.3	83.4	153.1	123.5
⁵**7**	1.836	1.687	2.167	1.864	1.756			82.7	96.7	139.9	123.4
C_s (curved)											
¹**5**	1.968	1.853		1.627		48.8	52.0		153.8		
D_{3h} (bipyramidal)											
¹**4**	1.827					91.2					
⁵**4**	1.867					77.6					

Raman spectroscopy. Rozhanskii *et al.* [13] assigned the doublet at 1031 cm^{-1} and 1024 cm^{-1} to the highest totally symmetric vibration of ¹**1**.

This interpretation was questioned by Andrews *et al.* [3] who investigated the reaction products by code-positing laser-evaporated aluminium atoms with Ar and $^{16,18}O_2$ at 11 K. Annealing of the argon matrix to 25 K led to a substantial increase of an IR band at 1211.2 cm^{-1}. Following Andrews *et al.* [3] this band and the corresponding sextet for the mixed isotopic oxygen reaction product belongs to a species with two equivalent and one non-equivalent oxygen atom. They assign these bands to ¹**1** and its isotopomers.

Al_2O_3 was also studied by anion photoelectron spectroscopy by Desai *et al.* [4]. $Al_2O_3^{\cdot-}$ is produced in the plasma reaction $Al + O_2$ in the presence of helium carrier gas followed by a supersonic expansion. After mass selection $Al_2O_3^{\cdot-}$ is subjected to photodetachment experiments at different wavelengths. Three bands were identified in the spectra of neutral Al_2O_3 and interpreted in terms of a ground state structure with a totally symmetric vibrational wave number of 850 ± 80 cm^{-1} and two excited electronic states thereof at 0.61 ± 0.02 eV and at 1.19 ± 0.08 eV. The authors designate these states to the singlet species ¹**2**, ¹**1**, and ¹**3** based on which they interpret their data. They arrive at the conclusion that the ground state of neutral Al_2O_3 must have a kite-shaped geometry.

From the results of our frequency calculations at the MP2 level of theory we assign the observed IR-active vibrations at 1170 ± 50 cm^{-1} to the σ_u^+ normal mode of ¹**1** at 1170 cm^{-1}. The Raman-active vibrations at 1031 cm^{-1} and 1024 cm^{-1} fit nicely with the σ_g^+ normal mode of ¹**1** at 1068 cm^{-1}.

We cannot support the assignment of the IR-active band at 502 cm^{-1} to ¹**1** [12] which is perfectly in line with the interpretation of the IR spectrum of Al_2O_3 as given by Andrews *et al.* [3]. A designation of the a_2'' normal mode at 543 cm^{-1} of ¹**4**, having the largest A_k value, to this IR band can only be conjectured. Moreover we have no indication for a species of C_1 symmetry at 964 cm^{-1} [12]. Neither the calculated spectrum of ¹**1** nor the spectra of the other two low-energy isomers of Al_2O_3, ³**2** and ¹**2** have IR-active normal modes within the interval from 900−1000 cm^{-1}.

We explain the vibrational fine structure of the photoelectron spectroscopic experiment with the additional presence of ³**2**. Therefore we rather assign the a_1 normal mode of 890 cm^{-1} of the triplet structure ³**2** to the experimentally observed band at 850 ± 80 cm^{-1} than the a_1 normal vibration of 807 cm^{-1} of the singlet species ¹**2**. There are three other normal modes within the same wave number range that could be contemplated *viz.* b_2 at 870 cm^{-1} (¹**2**), σ_u^+ at 872 cm^{-1} (¹**1**), and a_1 at 837 cm^{-1} (¹**3**). But the first two are not totally symmetric and the third definitely does not belong to a possible ground state structure. The energetically lowest state observed in the PES spectrum by Desai *et al.* [4] could be due to this triplet ³**2** species, which has a kite-shaped geometry and whose energy is only slightly (0.08 eV) lower than the linear ¹**1** isomer. The states which lie by 0.61 eV and 1.19 eV higher would then correspond to the isomers ¹**2** and ¹**3**, respectively, resulting in the energy state sequence of (³**2**, ¹**1**), ¹**2**, and ¹**3**. According to our MP2 results these energy differences between (³**2**, ¹**1**) and ¹**2** or ¹**3** amount to 0.84 and 1.52 eV. Furthermore we expect a positive electron affinity for the open-shell species ³**2**.

This triplet species was probably also generated in the process $Al + {}^{16,18}O_2$ studied by Andrews *et al.* [3]. Upon

annealing they observed a substantial increase not only for the band at 1211.2 cm^{-1} but as well for a strong band at 886.5 cm^{-1}. The authors did not structurally assign the latter. They further report an additional increasement in intensity of another IR-active band at 778 cm^{-1} upon annealing. This band may tentatively be interpreted by the b_2 normal mode of ^{3}**2** at 744 cm^{-1}.

4 Concluding remarks

The Al$_2$O$_3$ system exhibits a great variety of low-lying stationary points. Apart from singlet species there are also higher spin structures which are equally strongly bound and have not been antecedently considered. In total we localised 13 stationary points that can be assorted to 7 geometric nuclear configurations. The calculated energies and normal modes (MP2) explain readily the few available spectroscopic data on free or matrix isolated Al$_2$O$_3$. For an adequate description of the molecule it is infallibly necessary to include electron correlation.

References

1. V.G. Solomonik, V.V. Sliznev, Russ. J. Inorg. Chem. **32**, 788 (1987).
2. A.V. Nemukhin, F. Weinhold, J. Chem. Phys. **97**, 3420 (1992).
3. L. Andrews, T.R. Burkholder, J.T. Yustein, J. Phys. Chem. **96**, 10182 (1992).
4. S.R. Desai, H. Wu, C.M. Rohlfing, L.S. Wang, J. Chem. Phys. **106**, 1309 (1997).
5. E.G. Wolff, C.B. Alcock, Trans. Brit. Ceram. Soc. **61**, 667 (1962).
6. C.B. Alcock, M. Peleg, Trans. Brit. Ceram. Soc. **66**, 217 (1967).
7. H. Yanagida, F.A. Kröger, J. Am. Ceram. Soc. **51**, 700 (1968).
8. V.E. Henrich, P.A. Cox, *The Surface Science of Metal Oxides* (Cambridge University Press, New York, 1994).
9. R.P. Burns, J. Chem. Phys. **44**, 3307 (1966).
10. D.L. Hildenbrand, Chem. Phys. Lett. **20**, 127 (1973).
11. S. Sonchik, L. Andrews, K.D. Carlson, J. Phys. Chem. **87**, 2004 (1983).
12. I.L. Rozhanskii, G.V. Chertikhin, L.V. Serebrennikov, V.F. Shevelkov, Russ. J. Phys. Chem. **62**, 1215 (1988).
13. I.L. Rozhanskii, L.V. Serebrennikov, A.F. Shevelkov, Russ. J. Phys. Chem. **64**, 276 (1990).
14. T.S. Zyubina, Russ. J. Inorg. Chem. **30**, 1097 (1985).
15. V.G. Solomonik, I.G. Sazonova, Russ. J. Inorg. Chem. **30**, 1100 (1985).
16. J.M. Dyke, M. Feher, M.P. Hastings, A. Morris, A.J. Paul, Mol. Phys. **58**, 161 (1986).
17. J. Rubio, J.M. Ricart, F. Illas, J. Comp. Chem. **9**, 836 (1988).
18. J. Masip, A. Clotet, J.M. Ricart, F. Illas, J. Rubio, Chem. Phys. Lett. **144**, 373 (1988).
19. P. Joyes, *Les agrégats inorganiques élémentaires* (Les Éditions de Physique, Les Ulis, 1990, in French).
20. A.I. Boldyrev, P.v.R. Schleyer, J. Am. Chem. Soc. **113**, 9045 (1991).
21. L. Bencivenni, M. Pelino, F. Ramondo, J. Mol. Struct. **253**, 109 (1992).
22. A.V. Nemukhin, J. Almlöf, J. Mol. Struct. **253**, 101 (1992).
23. A.V. Zaitsevskii, G.V. Chertikhin, L.V. Serebrennikov, N.F. Stepanov, J. Mol. Struct. **280**, 291 (1993).
24. A.V. Nemukhin, J. Mol. Struct. **315**, 225 (1994).
25. E.F. Archibong, R. Sullivan, J. Phys. Chem. **99**, 15830 (1995).
26. R.D. Srivastava, M. Farber, Chem. Rev. **98**, 627 (1978).
27. S. Ciraci, I.P. Batra, Phys. Rev. B **28**, 982 (1983).
28. I.S. Kulikov, *Termodinamika Oksidov* (Metallurgiya Spravochnik, Moskva, 1986, in Russian).
29. A. Petzold, J. Ulbricht, *Aluminiumoxid* (Deutscher Verlag für Grundstoffindustrie, Leipzig, 1991, in German).
30. M. Catti, G. Valerio, R. Dovesi, M. Causà, Phys. Rev. B **49**, 14179 (1994).
31. C.W. Allen, *Astrophysical Quantities* (Athlone Press, London, 1973).
32. B.T. Draine, Ap. Space Sci. **65**, 313 (1979).
33. T. Kozasa, H. Hasegawa, Prog. Theor. Phys. **77**, 1402 (1987).
34. A.W. Irwin, Astron. Astrophys. Suppl. Ser. **74**, 145 (1988).
35. E. Sedlmayr, in *Interstellar Dust, IAU Symp. No. 135*, edited by L.J. Allamandola, A.G.G.M. Tielens (Kluwer, Dordrecht, 1989), p. 467-477.
36. B. Begemann, J. Dorschner, Th. Henning, H. Mutschke, J. Gürtler, C. Kömpe, R. Nass, Astrophys. J. **476**, 199 (1997).
37. L.R. Nittler, C.M.O.D. Alexander, X. Gao, R.M. Walker, E. Zinner, Astrophys. J. **483**, 475 (1997).
38. T. Bernatowicz, E. Zinner (eds.), *Astrophysical Implications of the Laboratory Study of Presolar Materials, AIP Conf. Proc. No. 402* (AIP Press, Woodbury, 1997).
39. M.J. Frisch, G.W. Trucks, M. Head-Gordon, P.M. Gill, M.W. Wong, J.B. Foresman, B.G. Johnson, H.B. Schlegel, M.A. Robb, E.S. Replogle, R. Gomperts, J.L. Andres, K. Raghavachari, J.S. Binkley, C. Gonzalez, R.L. Martin, D.J. Fox, B.J. Defrees, J.J.P. Stewart, J.A. Pople, Gaussian92/DFT (Gaussian Inc., Pittsburgh PA, 1992).
40. W.J. Hehre, L. Radom, P.v.R. Schleyer, J.A. Pople, *Ab Initio Molecular Orbital Theory* (Wiley, New York, 1986) (and references therein).
41. J.B. Foresman, A.E. Frisch, *Exploring Chemistry with Electronic Structure Methods* (Gaussian Inc., Pittsburgh PA, 1996), p. 64.
42. M. Costes, C. Naulin, in *Molecules in the Stellar Environment, Proc. IAU Coll. No. 146*, edited by U.G. Jørgensen (Springer, Berlin, 1994), p. 250-264.
43. M.W. Chase Jr., C.A. Davies, J.R. Downey Jr., D.J. Frurip, R.A. McDonald, A.N. Syverud, J. Phys. Chem. Ref. Data **14** Suppl. **1**, National Bureau of Standards (1985).
44. K.P. Huber, G. Herzberg, *Molecular Spectra and Molecular Structure, Vol. VI. Constants of Diatomic Molecules* (Van Nostrand Reinhold, New York, 1979).
45. T.U. Helgaker, J. Gauss, P. Jørgensen, J. Olsen, J. Chem. Phys. **106**, 6430 (1997).